01

Second harmonic generation via excitation of the surface modes of a one-dimensional photonic crystal

© V.N. Konopsky, A.A. Melnikov, E.V. Alieva, S.V. Chekalin

Institute of Spectroscopy RAS,
Troitsk, Moscow, Russia

e-mail: konopsky@isan.troitsk.ru

Received May 15, 2024
Revised June 29, 2024
Accepted August 01, 2024

A multilayer structure is presented that sustains propagation of two optical surface waves, one at the fundamental frequency and one at the second harmonic frequency, with the same effective refractive indices at both frequencies. Phase matching of these two surface waves and localisation of the field maxima at the layer boundaries allow us to observe generation of the second harmonic, despite the fact that the structure is composed of centrosymmetric materials, for which the second-order nonlinear susceptibility vanishes in the electric dipole approximation.

Keywords: multilayer structure, photonic crystal, surface optical waves, second harmonic generation.

DOI: 10.61011/EOS.2024.08.60026.6684-24

1. Introduction

To describe nonlinear optical effects, optical polarization of a medium **P** is usually expanded as Taylor series in the applied optical electric field strength **E** [1,2]:

$$\mathbf{P} = \chi^{(1)}\mathbf{E} + \chi^{(2)}\mathbf{E}^2 + \chi^{(3)}\mathbf{E}^3 + \dots \quad (1)$$

Here $\chi^{(1)}$ is the linear susceptibility contributing to the ordinary refractive index of a medium ($n^2 = 1 + 4\pi\chi^{(1)}$); $\chi^{(2)}$ is the second-order susceptibility describing such processes as sum frequency and second harmonic generation (SHG); $\chi^{(3)}$ is the third-order susceptibility describing, for example, the third harmonic generation and intensity-dependent refractive index.

The Taylor expansion is possible because optical field strengths are usually much lower than intra-atomic field strengths and the nonlinear susceptibilities $\chi^{(i)}$ are extremely low for $i > 1$. One of the ways to increase the nonlinear susceptibility (in particular, the coefficient $\chi^{(3)}$) in planar systems was proposed by V.M. Agranovich [3] and is based on the use of hybrid organic semiconductor structures. Agranovich showed that a considerable increase in $\chi^{(3)}$ can be achieved both in strongly-coupled hybrid systems [4] and in weakly-coupled hybrid systems [5].

Besides the enhancement of nonlinear susceptibility, for the experimental observation of nonlinear optical effects such as optical harmonic generation, the optimized design of the planar structures is also important in order to ensure phase matching of interacting waves at multiple optical frequencies. Thus, in our study [6] carried out under the supervision of V.M. Agranovich within his project supported by the Russian Foundation for Basic Research, third harmonic generation was observed in a one-dimensional photonic crystal (PC) that sustains propagation of in-phase optical surface waves both at the pumping wavelength of 1230 nm and the third harmonic wavelength of 410 nm.

Phase matching is particularly important for the observation of a nonlinear signal, if the nonlinear susceptibility coefficients are close to zero due to the symmetry of a material as is the case, for example, for $\chi^{(2)}$ in media with a center of inversion. In the present work we demonstrate the results of experiments on the second harmonic generation in a PC composed of centrosymmetric materials. Since the PC is designed in such a way that it supports in-phase optical surface modes both at the pumping wavelength of 1300 nm and at the second harmonic wavelength of 650 nm, the detection of a spatially coherent second-harmonic beam becomes possible despite the small value of $\chi^{(2)}$ due to the central symmetry.

2. Second harmonic generation in centrosymmetric materials

In centrosymmetric media, SHG is strictly forbidden in the electric dipole approximation. Because in this case $\mathbf{P}(-\mathbf{E}) = -\mathbf{P}(\mathbf{E})$ in materials with a center of inversion, then from (1) it follows that $\chi^{(2)}$ as well as all susceptibility coefficients at even powers of **E** should be zero. Nevertheless, weak sources of the second harmonic signal may occur even in such media provided that the symmetry of system is broken and reduced. For example, Reineker, Agranovich and Yudson [7] addressed the possibility of SHG in a centrosymmetric matrix containing an additional small number of charge-transfer complexes that reduce the symmetry of the system and make $\chi^{(2)}$ non-zero.

A better known example of system symmetry reduction contributing to SHG in centrosymmetric materials is the presence of a medium boundary as well as of other (internal) interfaces separating the materials, though being centrosymmetric, but having different refractive indices. This effect was investigated as early as in the 1960s [8] at the very beginning of nonlinear optical studies. Detailed historical reviews of nonlinear optics are provided in [9,10].

SHG in centrosymmetric media is described using a widely applicable model [11–13], in which the nonlinear response is separated into a surface (interface) dipole contribution resulting from the symmetry breaking at the interface between two media and a bulk contribution from multipoles beyond the electric dipole approximation:

$$\mathbf{P}_{NL} = \mathbf{P}_S + \mathbf{P}_V. \quad (2)$$

Wherein, when the surface component $\mathbf{P}_S$ is proportional to the squared optical electric field strength, then the bulk component $\mathbf{P}_V$ is proportional to the field multiplied by its spatial derivatives [1,11–14]:

$$\mathbf{P}_V = \delta(\mathbf{E}\cdot\nabla)\mathbf{E} + \beta\mathbf{E}(\nabla\cdot\mathbf{E}) + \gamma\nabla(\mathbf{E}\cdot\mathbf{E}). \quad (3)$$

The first two terms here correspond to the electric quadrupole contribution and the last one corresponds to the magnetic dipole contribution. δ, β and γ are constants that depend on the properties of the centrosymmetric medium. Note that the multipole contribution (beyond the electric dipole approximation) can be appreciable only in the case of a high electric field gradient and that such gradients (discontinuities) of the normal electric field component occur when the p-polarized wave travels through the interface (this results from the fact that the normal component of the electric displacement $D_n = \varepsilon E_n$ is continuous when there are no free charges at the interface).

2.1. Second harmonic generation during propagation of surface waves

In order to observe such weak nonlinear effects at an interface, it would be extremely helpful to localize spatially the radiation intensity in the vicinity of the studied interface. Therefore, optical surface waves are widely used for the investigation of nonlinear effects at the surface. Thus, for example, SHG at the air-to-silver interface upon excitation of surface plasmon polaritons along this interface was first observed in [15] using the Kretschmann configuration.

The experimental studies of surface polaritons, here, in at the Institute of Spectroscopy, began in 1974 following a suggestion of V.M. Agranovich, who had already written a review on the subject [16]. Many experimental studies in this field were carried out in the institute afterwards, including also the studies of nonlinear effects involving surface waves. For example, the second harmonic emitted perpendicularly to the quartz crystal wafer was detected upon excitation of counter-propagating polaritons along the surface of this wafer [17]. In the experiments on a free-electron laser the second harmonic [18] as well as the sum frequency [19] were detected upon excitation of the surface polaritons.

Optical surface waves in the PC used in the present work represent a type of surface waves that are localized near the surface as a result of total internal reflection from the external medium at the one side and of the presence of PC band gap from another side. Such optical waves can be excited both by the s-, and p-polarized radiation at the interface between the planar one-dimensional PC and the external medium at any pre-defined frequency and with any effective refractive index by appropriately selecting the thickness of two double layers and thickness of the last truncated layer [20]. This type of surface waves was first studied both theoretically [21,22] and experimentally [23] in the 1970s. Excitation of such optical surface waves was demonstrated in the Kretschmann configuration twenty years later [24,25]. In recent years, optical surface waves in PC find increasingly wide application for the development of optical sensors [26–31], optical biosensors [32–39] and in other areas [40–45].

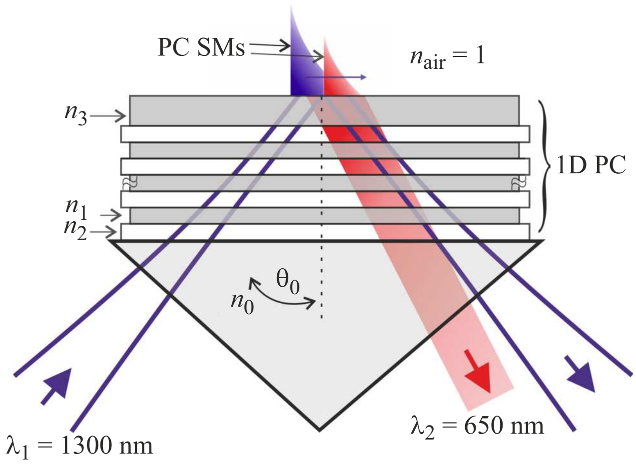

Figure 1. Experimental setup. PC SMs are PC surface modes, 1D PC is the one-dimensional PC (not to scale).

The possibility of flexible adjustment of both the excitation frequency and the effective refractive index of the optical surface waves of the PC makes them particularly attractive for harmonic generation. PCs for the third harmonic generation by the p-polarized radiation [6] and for the third harmonic generation by the s-polarized radiation [46] have been calculated and experimentally tested by us before. In the present work we have implemented a similar experimental setup as shown in Figure 1 with excitation of the p-polarized surface waves in the Kretschmann configuration, but of course with other thicknesses of PC layers calculated for the wavelengths of $\lambda_1 = 1300$ nm and $\lambda_2 = 650$ nm used in the present case.

2.2. Phase matching for two surface waves with multiple frequencies

Effective nonlinear conversion requires that the interacting optical waves maintain a fixed phase relationship during propagation through the medium despite its dispersion. Phase matching using birefringence that is often used to compensate for dispersion is impossible in optically isotropic materials. For a PC with nonlinear layers, theoretical calculations of phase matching were performed for pump and second harmonic waves in the bulk near the band gap edge [47]. In the present work we demonstrate a one-dimensional PC that supports propagation of optical waves along its surface both at the fundamental and the doubled frequency. The advantage of such a structure is that effective refractive indices for these two surface waves are equal to each other and approximately equal to the refractive index of air at both frequencies.

In the present work we used the following planar one-dimensional PC structure: prism/$(HL)^{14}H'$/air, where H is the TiO_2 layer (thickness $d_2 = 192.0$ nm), L is the SiO_2 layer ($d_1 = 222.1$ nm) and H' is the final TiO_2 layer ($d_3 = 231.0$ nm). The prism was made of fused quartz. The structure consisting of 29 TiO_2/SiO_2 layers (with TiO_2 as the first and last layers) was grown directly on the prism base using the plasma ion assisted electron beam vapor deposition method. Refractive indices of the SiO_2, TiO_2 layers and air at $\lambda_1 = 1300$ nm are $n_1 = 1.48$, $n_2 = n_3 = 2.268$ and $n_{\text{air}} = 1.0003$, respectively. This one-dimensional PC design supporting two optical modes at $\lambda_1 = 1300$ nm and $\lambda_2 = 650$ nm was calculated using the computer program available for free at [48].

The results of the theoretical calculation of the dispersion of the fabricated one-dimensional PC are shown in Figure 2. The dispersion is represented as the logarithm of the optical field enhancement factor (i.e. $\log_{10}[I_e/I_0]$) in the external medium in the vicinity of the structure in the 1/lambda(rho) coordinates. $1/\lambda(\rho)$. The band gaps of the PC are shown as dark-blue regions with the enhancement much lower than 1. Optical surface modes are shown as red curves with the enhancement of about 100 located within the band gaps. The angular parameter $\rho = n_0 \sin\theta_0 = 1.01$ for which the surface mode is excited is equal to the effective refractive index of the surface mode.

Figure 2 shows that the calculated structure has two band gaps at 1300 nm and 650 nm, and both band gaps contain surface waves. For phase matching of these surface waves, their effective refractive indices must coincide in some range at the fundamental and doubled frequencies. This is the case at $\rho = n_{\text{eff}} = 1.01$ (see the vertical white dashed line in Figure 2). Therefore, when the PC surface mode is excited at the wavelength$\lambda_1 = 1300$ nm with $\rho = 1.01$, generation of its second harmonic may be expected at the wavelength$\lambda_1 = 650$ nm with the same effective refractive index.

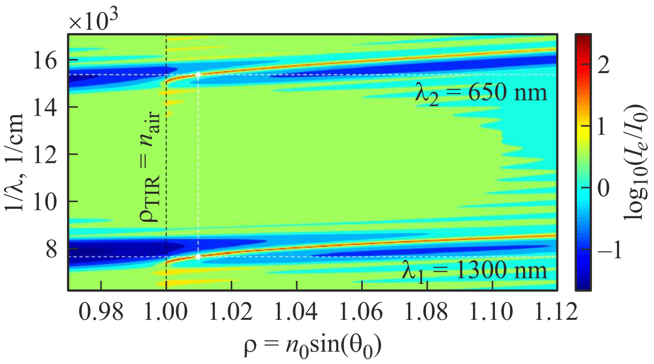

Figure 2. Calculated PC dispersion for the p-polarized radiation. Phase matching points at $\rho = 1.01$ are marked by white rhombs and connected by a vertical white dashed line.

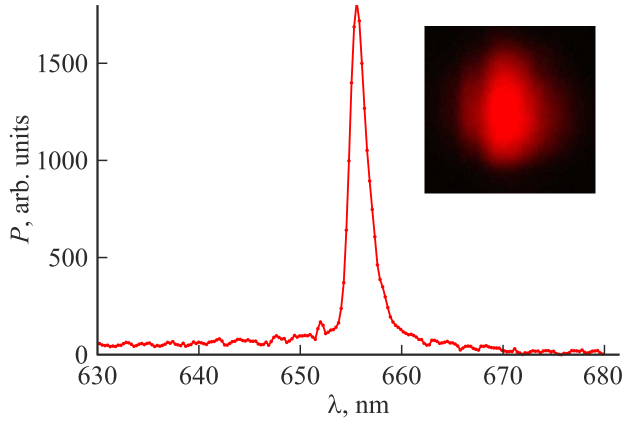

Figure 3. Spectrum of the second harmonic radiation. The inset shows a photograph of the second harmonic beam on a paper screen made in darkness.

3. Experimental results

Femtosecond pulses at the wavelength$\lambda_1 = 1300$ nm were generated by a parametric amplifier (Topas, Light Conversion Ltd.) pumped by the radiation of a titanium-sapphire regenerative amplifier (Spitfire Pro, Spectra Physics) at the repetition rate of 1 kHz. Signal and idler beams were separated using a specialized wavelength separator (Light Conversion Ltd.). After that, the signal beam was transmitted through an achromatic half-wave plate and a continuously variable neutral density filter (Thorlabs) to prepare the 100 fs p-polarized pulses with the wavelength $\lambda_1 = 1300$ nm incident on the prism. The second harmonic wave that had excited the surface mode at the wavelength$\lambda_2 = 650$ nm was reradiated back into the prism while travelling on the external surface of the PC as shown in Figure 1.

Such method of phase matching on the external surface of the SiO_2/TiO_2 multilayer structure differs from the approach described in [49,50], where phase matching occurred between the fundamental mode of a conventional waveguide (with the total internal reflection on both boundaries) and the second harmonic of the waveguide mode from the PC, in that both interacting modes in the former case are surface modes located in the band gaps of different orders and both modes have effective refractive indices close to the refractive index of air.

The spectrum of the second harmonic radiation outgoing from the prism is shown in Figure 3. The spectrum was acquired within 100 ms. It was recorded at femtosecond excitation with an average power of 27 mW and repetition rate of 1 kHz. This pumping wave was weakly focused by a lens with a focal distance of 300 mm onto the PC surface through the Kretschmann prism. The size of the outgoing second harmonic beam shown in the inset to Figure 3 is about 1.5 mm at a distance of 500 mm from the prism.

To ensure that the observed signal was generated in a second-order nonlinear process, we have measured the dependence of the power of the second harmonic signal on the femtosecond pump power. This dependence is shown in Figure 4 on a logarithmic scale, where the slope of the fitting line is2.0 ± 0.2. SHG efficiency at the maximum pumping power $P_{1st}^{max} = 27$ mW was $2 \cdot 10^{-9}$.

4. Discussion

Band gaps are known to occur in a periodic structure due to multiple reflections in periodic layers that leads to destructive light interference. Standing optical waves with the same wave vector and, consequently, with the same period of the standing wave in such media can have two mode configurations: one configuration, when the standing wave forms an optical field with maxima in layers with the higher refractive index and the other configuration, when the standing wave forms maxima in layers with the lower refractive index. The difference in the refractive indices of these two configurations means that they have different energies and, consequently, different frequencies (for the same wave vector), i.e. a gap occurs on the dispersion curve of the bulk mode — and this is how the forbidden frequency band is formed in the spectrum. This effect is graphically illustrated in figures in [51].

It is important for the present case that, though light propagation at frequencies in the band gap is forbidden, optical surface waves can nevertheless exist within the band gap. Consequently, when the surface waves are excited in the vicinity of the band gap, they will have field strength maxima at the interface between the layers with high and low refractive indices, rather than within these layers. The main field strength maximum will be localized at the external boundary and the other maxima will be located on the interfaces of the centrosymmetric media inside the PC. Moreover, for the p-polarized wave, the normal field component will have discontinuities on all interfaces, i.e. near these field maxima. Therefore, besides the electric dipole contribution to the nonlinearity (the term $\mathbf{P}_S$ in (2)) resulting from the symmetry breaking on interfaces, in such a system, according to equation (3), contributions can also appear from multipoles that are proportional to the field gradient multiplied by the field strength. The field structure in our PC upon excitation of the surface resonance at $\rho = 1.01$ for $\lambda_1 = 1300$ nm is shown in Figure 5. Discontinuities of the maxima of the normal filed component on all interfaces are clearly visible. Quantitative estimation of different contributions to SHG from equations (2) and (3) in such a system requires a separate study.

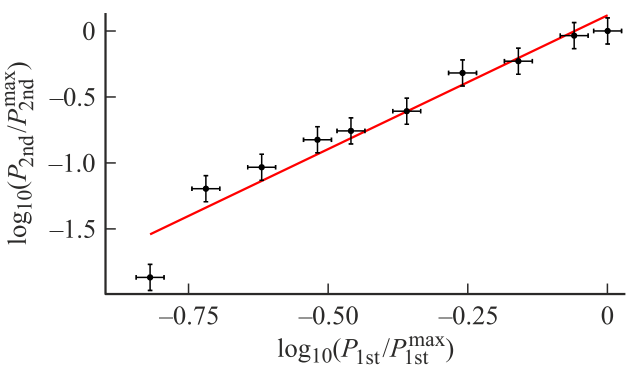

Figure 4. Dependence of the power of the second harmonic signal on the pump beam power (circles). Solid curve — linear approximation of the experimental points on a logarithmic scale with a slope of 2.0 ± 0.2.

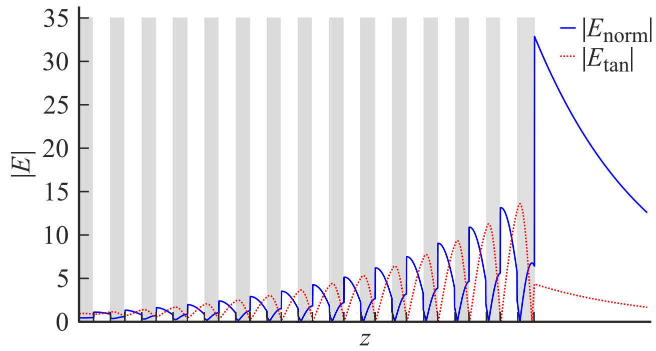

Figure 5. Spatial distribution of the tangential and normal components of the p-polarized optical field for $\lambda_1 = 1300$ nm at $\rho = 1.01$.

5. Conclusion

Second harmonic generation was demonstrated using optical surface modes of the one-dimensional PC, where the fundamental and the second harmonic frequencies are in resonance with the corresponding optical surface modes. Three key properties of the presented PC structure increase the SHG efficiency in centrosymmetric media (that is extremely low otherwise):

1. near-surface localization and enhancement of the optical field due to the excitation of the optical surface wave;

2. phase matching between the first and the second harmonics of the optical surface waves, when they have the same effective refractive index that is close to 1 (i.e. close to the refractive index of the external medium — air in our case);

3. field maxima and gradients are localized on the interfaces between the layers of centrosymmetric materials.

Thus, we have developed a multilayer structure that allows one to routinely obtain the second harmonic signal from interfaces between centrosymmetric media. Such structure can be used for experimental verification of polarization and anisotropy of two-dimensional materials deposited onto its surface.

Acknowledgments

The authors are grateful to the Russian Science Foundation (grant № 22-22-00836) and the Institute of Spectroscopy RAS (topic № FFUU-2022-0003) for support.

Conflict of interest

The authors declare that they have no conflict of interest.

References

[1] Y.-R. Shen, *Principles of Nonlinear Optics* (Wiley-Interscience, New York, NY, USA, 1984).
[2] R.W. Boyd, *Nonlinear Optics* (Academic Press, San Diego, 1992).
[3] V. Agranovich, Y.N. Gartstein, M. Litinskaya, Chemical Reviews **111**, 5179 (2011).
[4] V. Agranovich, D. Basko, G. La Rocca, F. Bassani, Journal of Physics: Condensed Matter **10**, 9369 (1998).
[5] V. Agranovich, G.C. La Rocca, Journal of Luminescence **169**, 422 (2016).
[6] V.N. Konopsky, E.V. Alieva, S.Y. Alyatkin, A.A. Melnikov, S.V. Chekalin, V.M. Agranovich, Light: Science & Applications **5**, e16168 (2016).
[7] P. Reineker, V. Agranovich, V. Yudson, Chemical Physics Letters **260**, 621 (1996).
[8] N. Bloembergen, P. Pershan, Physical Review **128**, 606 (1962).
[9] N. Bloembergen, Applied Physics B **68**, 289 (1999).
[10] Y. Shen, IEEE Journal of Selected Topics in Quantum Electronics **6**, 1375 (2000).
[11] N. Bloembergen, R.K. Chang, S. Jha, C. Lee, Physical Review **174**, 813 (1968).
[12] D. Epperlein, B. Dick, G. Marowsky, G. Reider, Applied Physics B **44**, 5 (1987).
[13] T. Heinz, H. Ponath, G. Stegeman, by H.-E. Ponath and GI Stegeman (Elsevier Science Publishers BV, Amsterdam, 1991) p. 353 (1991).
[14] Y. Shen, F. deMartini, in *Surface Polaritons*, edited by V. Agranovich, D. Mills (Elsevier, 1982), vol. 1 of *Modern Problems in Condensed Matter Sciences*, pp. 629–660.
[15] H. Simon, D. Mitchell, J. Watson, Physical Review Letters **33**, 1531 (1974).
[16] V. M. Agranovich, Soviet Physics Uspekhi **18**, 99 (1975).
[17] E. Alieva, G. Zhizhin, V. Yakovlev, V. Sychugov, JETP Lett **62** (1995).
[18] G. Zhizhin, E. Alieva, L. Kuzik, V. Yakovlev, D. Shkrabo, A. Van der Meer, M. Van der Wiel, Applied Physics A: Materials Science & Processing **67** (1998).
[19] E. Van der Ham, Q. Vrehen, E. Eliel, V. Yakovlev, E. Alieva, L. Kuzik, J. Petrov, V. Sychugov, aA. Van Der Meer, JOSA B **16**, 1146 (1999).
[20] V. Konopsky, Coatings **12**, 1489 (2022).
[21] J.A. Arnaud, A.A.M. Saleh, Appl. Opt. **13**, 2343 (1974).
[22] P. Yeh, A. Yariv, C.-S. Hong, J. Opt. Soc. Am. **67**, 423 (1977).
[23] P. Yeh, A. Yariv, A.Y. Cho, Appl. Phys. Lett. **32**, 104 (1978).
[24] W.M. Robertson, M.S. May, Appl. Phys. Lett. **74**, 1800 (1999).
[25] A. Shinn, W. Robertson, Sens. Actuator B-Chem. **105**, 360 (2005).
[26] V.N. Konopsky, E.V. Alieva, Phys. Rev. Lett. **97**, 253904 (2006).
[27] V.N. Konopsky, E.V. Alieva, Opt. Lett. **34**, 479 (2009).
[28] S. Hamidi, R. Ramezani, A. Bananej, Optical Materials **53**, 201 (2016).
[29] D.O. Ignatyeva, G.A. Knyazev, P.O. Kapralov, G. Dietler, S.K. Sekatskii, V.I. Belotelov, Scientific Reports **6**, 28077 (2016).
[30] J. Li, T. Tang, Y. Zhang, L. Luo, P. Sun, Optik **155**, 74 (2018).
[31] D. Ignatyeva, P. Kapralov, P. Golovko, P. Shilina, A. Khramova, S. Sekatskii, M. Nur-E-Alam, K. Alameh, M. Vasiliev, A. Kalish, et al., Sensors **21**, 1984 (2021).
[32] V.N. Konopsky, E.V. Alieva, Anal. Chem. **79**, 4729 (2007).
[33] Y. Guo, J.Y. Ye, C. Divin, B. Huang, T.P. Thomas, J.R. Baker, Jr., T.B. Norris, Anal. Chem. **82**, 5211 (2010).
[34] V.N. Konopsky, T. Karakouz, E.V. Alieva, C. Vicario, S.K. Sekatskii, G. Dietler, Sensors **13**, 2566 (2013).
[35] P. Rivolo, F. Michelotti, F. Frascella, G. Digregorio, P. Mandracci, L. Dominici, F. Giorgis, E. Descrovi, Sensors and Actuators B: Chemical **161**, 1046 (2012).
[36] V.N. Konopsky, E.V. Alieva, Sensors and Actuators B: Chemical **276**, 271 (2018).
[37] M. Khodami, Z. Hirbodvash, O. Krupin, W. R.Wong, E. Lisicka-Skrzek, H. Northfield, C. Hahn, P. Berini, Journal of Microelectromechanical Systems **30**, 686 (2021).
[38] B. Kalas, K. Ferencz, A. Saftics, Z. Czigany, M. Fried, P. Petrik, Applied Surface Science **536**, 147869 (2021).
[39] R. Shakurov, S. Sizova, S. Dudik, A. Serkina, M. Bazhutov, V. Stanaityte, P. Tulyagin, V. Konopsky, E. Alieva, S. Sekatskii, et al., Polymers **15**, 2607 (2023).
[40] A. Delfan, M. Liscidini, J. E. Sipe, JOSA B **29**, 1863 (2012).
[41] N. R. Fong, M. Menotti, E. Lisicka-Skrzek, H. Northfield, A. Olivieri, N. Tait, M. Liscidini, P. Berini, ACS Photonics **4**, 593 (2017).
[42] I. Degli-Eredi, J. Sipe, N. Vermeulen, Optics Letters **40**, 2076 (2015).
[43] V. Konopsky, V. Prokhorov, D. Lypenko, A. Dmitriev, E. Alieva, G. Dietler, S. Sekatskii, Nano-Micro Letters **12**, 1 (2020).
[44] T. Kovalevich, D. Belharet, L. Robert, G. Ulliac, M.-S. Kim, H.P. Herzig, T. Grosjean, M.-P. Bernal, Applied Optics **58**, 1757 (2019).
[45] V. Konopsky, Sensors **23**, 8812 (2023).
[46] V. Konopsky, A. Melnikov, E. Alieva, S. Chekalin, JOSA B **36**, 2871 (2019).
[47] R. Zaporozhchenko, Optics and Spectroscopy **95**, 976 (2003).
[48] V. Konopsky (2022), https://www.pcbiosensors.com/1DPC4all.htm, Version 1.1.8401.20377.
[49] A. Helmy, Optics Express **14**, 1243 (2006).
[50] A. Arjmand, P. Abolghasem, J. Han, A.S. Helmy, JOSA B **32**, 577 (2015).
[51] W. L. Barnes, T. Preist, S. Kitson, J. Sambles, Physical Review B **54**, 6227 (1996).

Translated by E.Ilinskaya